processes

MDPI

Article

Octagonal Starfish-Inspired Roller Imprinting Control for Multi-Space and Multi-Axial Microstructure Replication

Yung-Jin Weng *, Yi-Xuan Zhong, Jin-Chen Guo and Zi-Jia Wang

Department of Mechanical and Energy Engineering, National Chiayi University, Chiayi 60004, Taiwan
* Correspondence: yjweng@mail.ncyu.edu.tw

Abstract

This study proposes a novel octagonal starfish-inspired roller imprinting control for multi-space and multi-axial microstructure replication, featuring a roller printing system with a controllable mold structure for multi-space and multi-axis applications. First, a microstructure was made and a micro mold was replicated to develop and simulate a negative Poisson ratio structure as a special structure to control the polymer microstructure mold. Meanwhile, a spatial axial roller imprinting system was designed as a roller imprinting replication system for the replication and roller imprinting of microstructures to research and conduct a roller imprinting testing experiment. The experiment results showed that the multi-space and multi-axial roll imprinting processing system with a controllable mold in this research had high replication formability. The results proved that the high replication formability of the microstructure obtained through white light scanning after subsequent roller imprinting was up to 98.75%. The diameter of the microstructure reached 99.025%, and the development of this innovative system and method of new technology could obtain the expected replication formability of the microstructure. Meanwhile, good achievements were obtained through optical preliminary validation. The results of this research could provide a reference about continuous microstructure component roll forming processing for academic and technological development.

Keywords: starfish-inspired; multi-axial; optical; microstructure; roller imprinting



Academic Editors: Constantin Alberto Hernández Bocanegra, José Ángel Ramos-Banderas and Gildardo Solorio Diaz

Received: 3 May 2025
Revised: 5 June 2025
Accepted: 12 June 2025
Published: 21 June 2025

Citation: Weng, Y.-J.; Zhong, Y.-X.; Guo, J.-C.; Wang, Z.-J. Octagonal Starfish-Inspired Roller Imprinting Control for Multi-Space and Multi-Axial Microstructure Replication. *Processes* **2025**, *13*, 1966. https://doi.org/10.3390/pr13071966

Copyright: © 2025 by the authors. Licensee MDPI, Basel, Switzerland. This article is an open access article distributed under the terms and conditions of the Creative Commons Attribution (CC BY) license (https://creativecommons.org/licenses/by/4.0/).

1. Introduction

Microstructure component fabrication technology is changing with each passing day. With the progress of science and technology, preparation and launching of flexible wearable microsystems have become the main development emphasis of current technology. Flexible display systems are dominated by macromolecular materials. Compared with other materials, this material is light-weight, easily processed, and of high light penetrability. Therefore, the continuous improvement of wearable microsystems, optical biomedicine, and display technology has also taken polymer materials as major development direction. The structure of the membrane in a flexible display system needs to adapt to diversified bending patterns. Meanwhile, special design planning to receive the light source through certain directions and angles and homogenize the light source is not necessary. Thus, mold preparation is extremely important. Microelectromechanical systems (MEMS) processing technology [1–3], laser processing technology [4–6], and special exposure and development technology were often adopted by previous research scholars to prepare molds [7–10]. Later, continuous roller imprinting and imprinting processing with prepared molds [11–15] were conducted to shape complementary microstructure components and obtain membranes

with microstructures. In 2019, Zong et al. [16] successfully utilized wet etching technology to fabricate a honeycomb array microstructure on polycrystalline silicon, featuring an aperture of 15.1 μm, a depth of 6.5 μm, and a period of 18 μm. This structure also exhibits low light reflectivity. In 2019, Lee et al. [17] developed a seamless microstructure patterning technique on the surface of a slender hollow roller system through repeated exposure and development, achieving feature sizes ranging from ten to more than ten microns. In 2017, Kang et al. [18] successfully fabricated MoS_2/graphene hybrid structure patterns using soft lithography technology. The above fabricating method often adopts a one-to-one method to fabricate materials through imprinting. This research proposed a roller imprinting system with a multi-space and multi-axial controllable mold structure and adopted a negative Poisson ratio structure to control the mold. This study predicted that continuous microstructure components fabricated through roller imprinting with rapid and controllable molds could be realized through this new processing technology method. This research hoped to provide a precise processing technology with high feasibility that could be successfully implemented during the development stage of a microsystem. This study introduces process innovation to significantly enhance the efficiency of microstructure soft molds and effectively eliminate redundant MEMS processing steps. This study contributes to reducing carbon emissions in manufacturing, substantially lowering production costs, and providing a significant boost to the sustainable optimization of modern automated manufacturing technologies. Furthermore, regarding the mold regulation control style proposed, the process system is compatible with digital intelligent control, aligning with the green manufacturing principles of Industry 4.0.

2. Structure Design and Control Mechanism of the Negative Poisson Ratio Material

2.1. Structure Design and Mechanical Property Test Using the Negative Poisson Ratio

This research designed a geometric structure controlled through a negative Poisson ratio, as shown in Figure 1. Meanwhile, a preliminary discussion and a comparison were conducted on the negative Poisson ratio of both metallic and polymer materials. Adjustable geometrical parameters were used as a parameter basis for the structure changes, of which single geometric structures were separately designed with a maximum range of 10 mm × 10 mm so as to change the geometrical parameters of all structures and obtain the Poisson ratio required by this research.

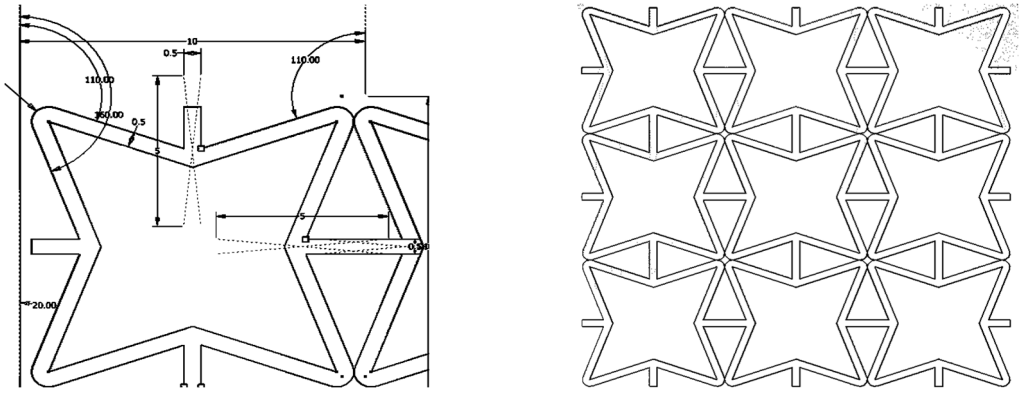


Figure 1. Geometric characteristics of the negative Poisson ratio control structure involved in this structure.

2.1.1. Analysis of NPR Geometric Structure of Metallic Materials and Analysis of the Design and Simulation of Junctions

This study used ANSYS to analyze and compare the geometric structure (3 × 3 arrays) and change in Poisson ratio during the stretching process of different materials. Three metallic materials were discussed according to their characteristics: (a) pure nickel (Ni), with an elastic modulus of 200 GPa, a Poisson ratio of 0.31, and a density of 8908 kg/m^3; (b) pure zinc (Zn), with an elastic modulus of 108 GPa, a Poisson ratio of 0.25, and a density of 7140 kg/m^3; and (c) pure magnesium (Mg), with an elastic modulus of 45 GPa, a Poisson ratio of 0.29, and a density of 1738 kg/m^3, as well as other conditions [19]. Meanwhile, the simulation analysis of the unequal stretched length showed that the Poisson ratio change of their geometric structures was stable. The Poisson ratio of the three metallic materials for the tensile elasticity analysis range was stabilized at −0.86 (−0.85 to −0.87), as shown in Table 1.

Table 1. Simulation and analysis of changes in the Poisson ratio with unequal tensile lengths of the metallic materials.

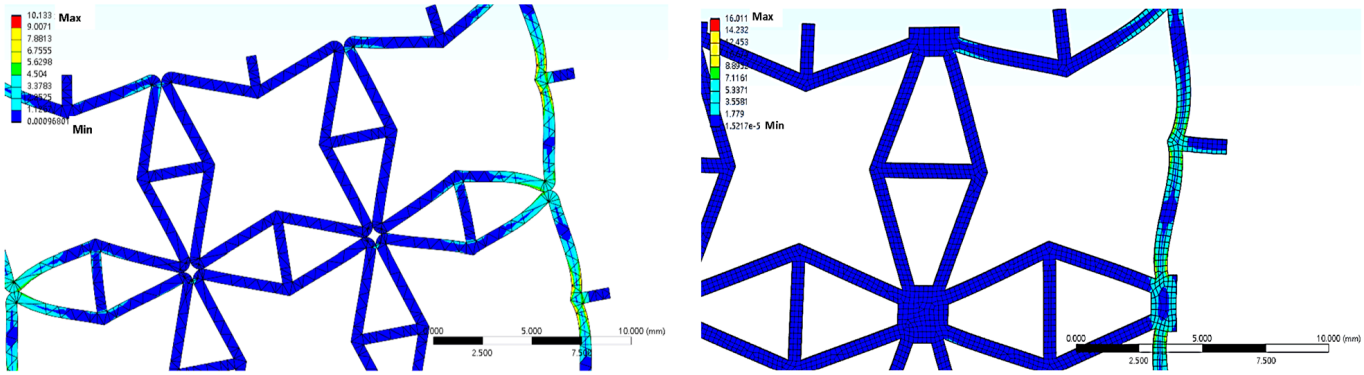
Materials	Stretch (mm)	Poisson's Ratio
Nickel (Ni)	0.02	−0.085
	0.06	−0.085
	0.1	−0.085
Zinc (Zn)	0.02	−0.086
	0.06	−0.086
	0.1	−0.086
Magnesium (Mg)	0.02	−0.085
	0.06	−0.085
	0.1	−0.085

2.1.2. Analysis of NPR Geometric Structure of Metallic Materials and Analysis of the Design and Simulation of Junctions

This study used ANSYS to analyze and compare the geometric structure (3 × 3 arrays) and change in Poisson ratio in the stretching process of macromolecular materials, including acrylonitrile butadiene styrene (ABS) and a thermoplastic elastomer (TPE). The material parameters for the simulation were a density of 950 kg-m^3, a Poisson ratio of 0.45, and a Yung's modulus of 2.24 GPa. This study analyzed the round and square junctions of the geometric structures to confirm the arrangement and optimal design approach for creating arrays the geometric structures. The results showed that the round design of the ABS material had better tensile resistance capability (Table 2, Figure 2).

Table 2. Simulated tensile stress and Poisson ratio performance with a fixed stretching length of ABS.

Shape / Materials	Acrylonitrile Butadiene Styrene (ABS)		
	Stretch Length (mm)	Tensile Stress (MPa)	Poisson's Ratio
Round	0.02	10.133	−0.038
Square	0.02	16.011	−0.056



(**a**) (**b**)

Figure 2. Simulated performance at the junctions of the geometric structure with 0.2 mm of stretching: (**a**) round design; (**b**) square design.

Under equal tensile conditions (a stretch of 0.1 mm from both left and right), the stress on the round design was smaller, indicating it had a larger stretch range and pull-out effect of resistance in the structure. The TPE also had the same performance. At the same time, the Poisson ratio (round design: −0.77, square design: −0.048) remained stable with the increase in tensile displacement. However, the Poisson ratio of the round design was larger, as shown in Table 3.

Table 3. Simulation and analysis of changes in the Poisson ratio with an unequal tensile length of TPE.

Shape / Materials	Thermoplastic Elastomer (TPE)	
	Stretch Length (mm)	**Poisson's Ratio**
Round	0.1	−0.077
	0.3	−0.077
	0.5	−0.077
Square	0.1	−0.048
	0.3	−0.048
	0.5	−0.048

2.2. Space Angle Adjustment Mechanism

This study adopted a multi-space and multi-axial angle method for adjustment, and a system table was independently developed for use. After multiple axes were connected in series through molds, microstructures on the molds could be adjusted through controlling the angular displacement. Meanwhile, driven by the NPR geometric structure, shape is controlled in addition to the form as an expression of structure. The horizontal displacement of the belt length of the system (at the central axis) over the roller was as shown in Figure 3.

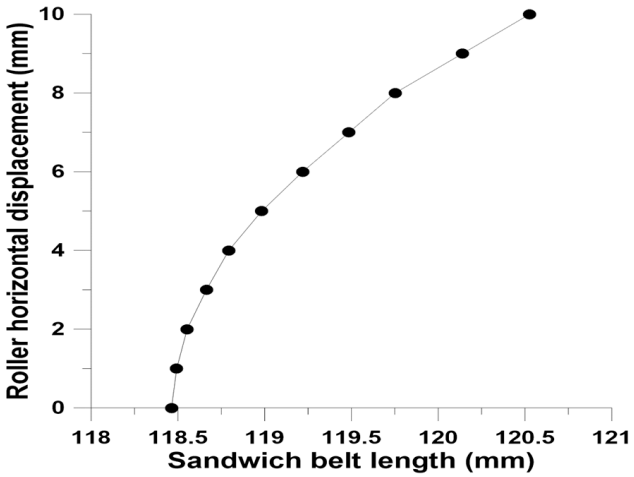


Figure 3. Horizontal displacement of the belt length of the system over roller.

3. Experimental Procedure

3.1. Design and Development of the Multi-Space and Multi-Axial Roller Imprinting System Controllable Mold Structure

This study designed a multi-space and multi-axial roller imprinting system with controllable a mold. A negative Poisson ratio structure with multi-space and multi-axial adjustment characteristics was adopted to obtain the features and shape required by the mold microstructure. The system contained an R2P roller imprinting and UV-light exposure platform mechanism, a multi-space and multi-axial adjustment and roller imprinting mechanism, a compound mold system with a driving mechanism, and a microstructure adjusted by the TPE structure. The imprinting platform utilizes quartz glass with high light transmittance and provides a UV light-curing photoresist. UV light employs short-wavelength, high-energy ultraviolet radiation as its primary exposure mechanism. Meanwhile, this research used a sandwich microstructure mold arranged on the multi-space and multi-axial controllable roller to adjust the imprinting processing, as shown in Figure 4.

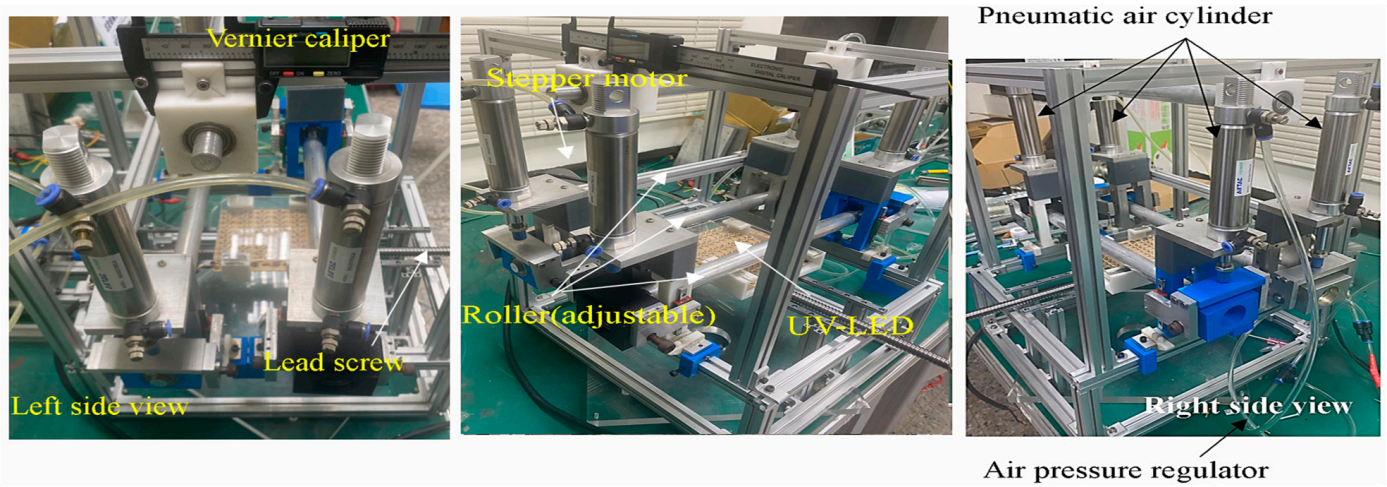


Figure 4. Multi-space and multi-axial roller imprinting system with controllable mold structure.

3.2. Selection and Preparation of the NPR Structure Mold, Microstructure Mold, and Photoresist Material

3.2.1. Selection of the NPR Structure Mold, Microstructure Mold, and Photoresist Material

The NPR structure was dominated by thermoplastic elastomer (TPE), which is characterized by elasticity and toughness. The simulation of its forequarter also showed mechanical properties and stable negative Poisson ratio performance that could meet the adjustment demand of this research; moreover, polydimethylsiloxane (PDMS; Sylgard™ 184, Dow Corning), was adopted as the microstructure mold material, and an SU8 UV-curing photoresist (Kayaku Advanced Materials, Inc., Westborough, MA, USA) was adopted as the photoresist.

3.2.2. Preparation of the NPR Structure Mold, Microstructure Mold, and Sandwich Microstructure Mold

The NPR structure of this research was an adjustable microstructure compound mold system using TPE as the polymer material. Preparation is mainly achieved with a three-dimensional printer station. The microstructure mold was prepared through laser machining of the array hole master, hot-pressing of the array's semicircular convex circle, and PDMS rollover of the array hole's semicircular concave circle, as shown in Figure 5.

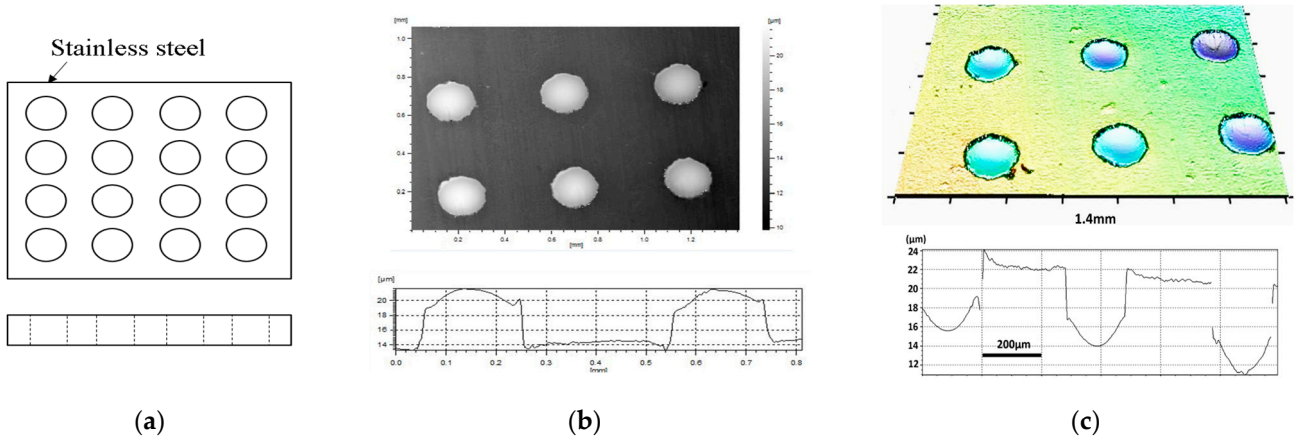
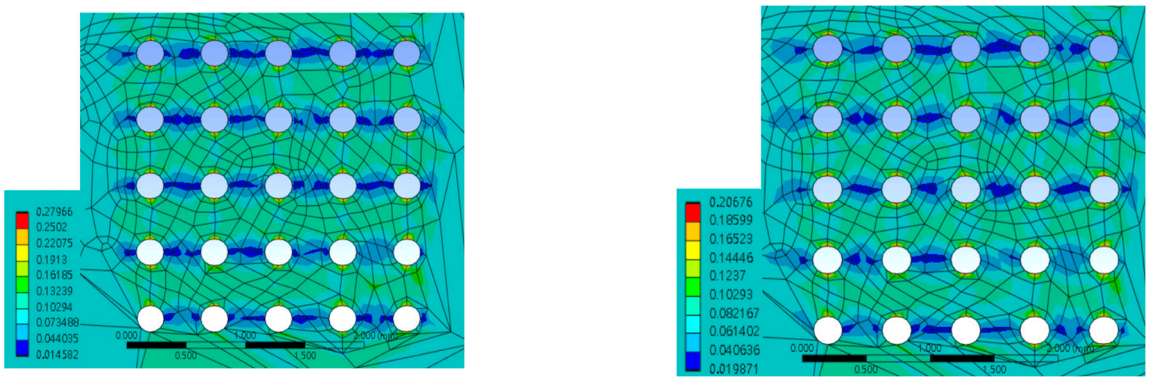


Figure 5. Preparation procedure of the microstructure mold: (**a**) laser machining the array hole master, (**b**) profile measurement of the array hemispherical convex circles through hot-pressing, and (**c**) array hole hemispherical concave circles through PDMS rollover.

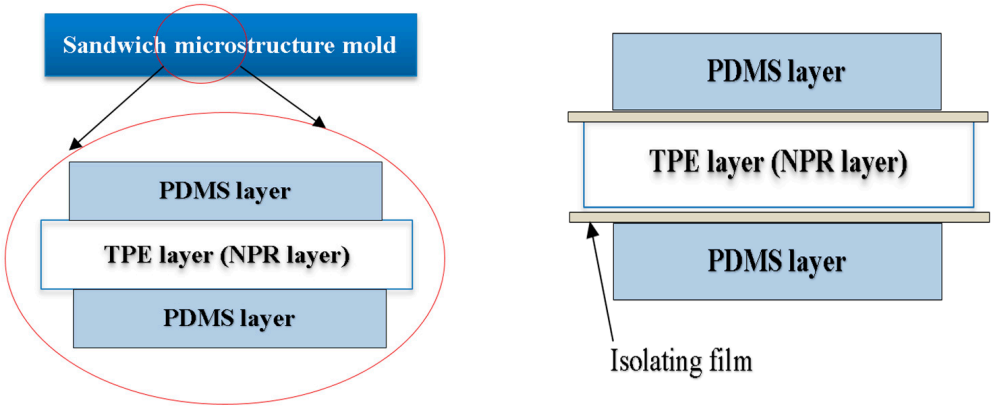
In addition, the Poisson ratio stress analysis and strain simulation analysis were conducted on a single microstructure of the PDMS. The experiment results showed that the average Poisson ratio of any single microstructure was 0.28 when the tensile displacement was within 1.5 mm, 2.5 mm, and 3.5 mm, as shown in Figure 6.

Additionally, preparation of the sandwich microstructure mold was conducted using superimposed cladding by driving a superimposed cladded PDMS microstructure mold layer through TPE polymer material in the intermediate layer (with high mechanical properties), as shown in Figure 7a. The intermediate layer was prefabricated and then an isolating film was swung into via the intermediate NPR structure layer and the PDMS structure layer (avoiding bonding of the upper and lower layer due to PDMS flow). The isolating film was removed after completion of preparation and curing to obtain the sandwich microstructure mold, as shown in Figure 7b.



(**a**) (**b**)

Figure 6. Simulation of stretching in a single microstructure: (**a**) stress; (**b**) strain.



(**a**) (**b**)

Figure 7. Preparation of the sandwich microstructure mold: (**a**) drive the superimposed cladded PDMS microstructure mold layer through the TPE polymer material in the intermediate layer (with high mechanical properties), the red circle indicate the stacking sequence of each layer of the sandwich microstructure mold insert; (**b**) removing the isolating film after completion of preparation and curing to obtain the sandwich microstructure mold.

3.3. Processing of the Multi-Space and Multi-Axial Roller Imprinting System with Controllable Mold

The research system was designed to handle adjustable multi-space and multi-axial positioning. The physical characteristics of the microstructure were obtained via adjusting the polymer NPR mold to execute continuous roll imprinting processing, as shown in Figure 8.

The steps of research system were: (a) build a sandwich microstructure mold suitable for research; (b) adjust the position of the roller to the physical characteristics of the microstructure mold within the elastic limit; (c) prepress and start continuous roller imprinting as well as UV-LED exposure and curing to realize continuous roll imprinting processing; (d) conduct real-time charge-coupled device (CCD) detection to the finished microstructure components synchronously and conduct fine-tuning adjustments on the finished microstructure components.

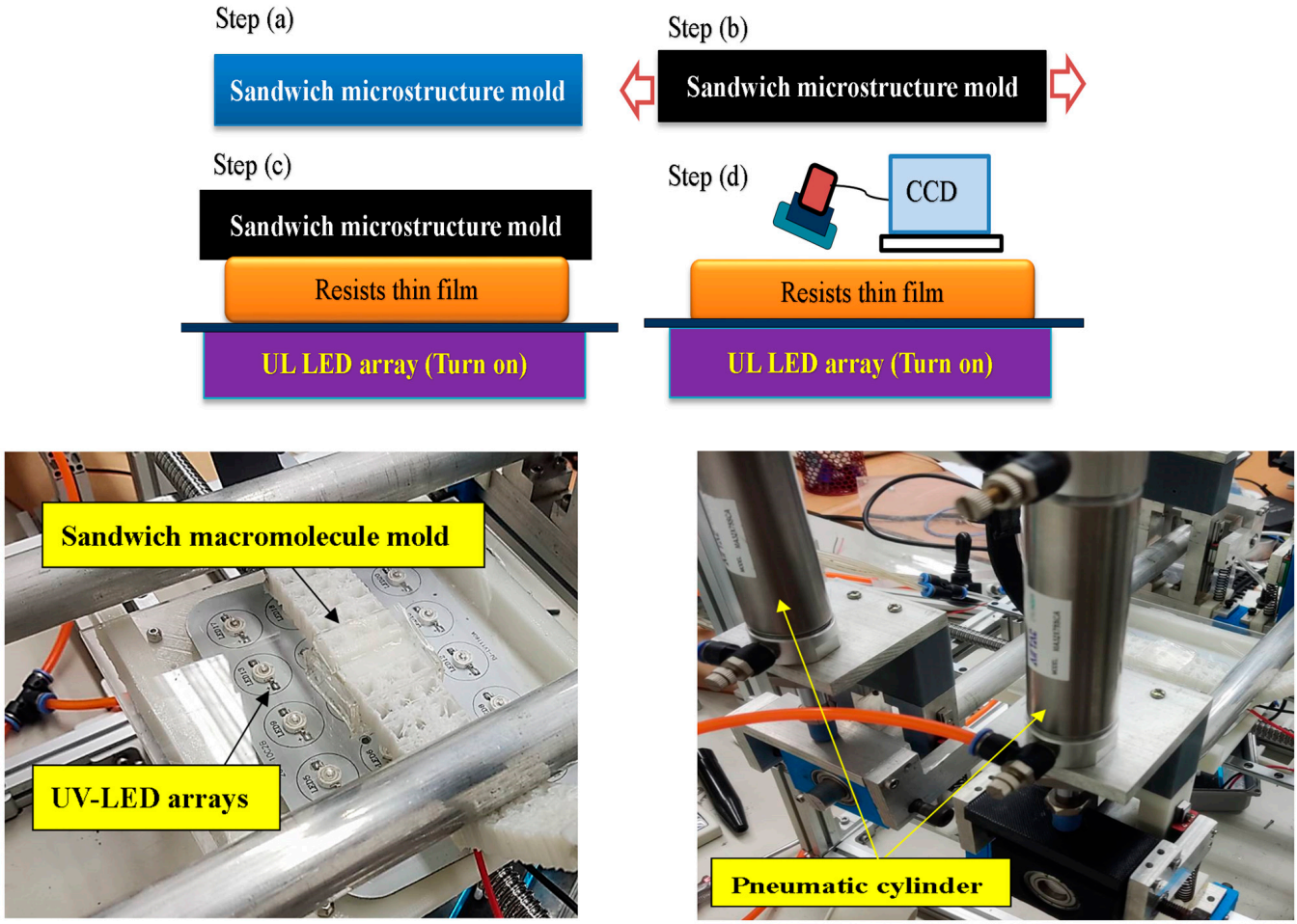


Figure 8. Processing step of the multi-space and multi-axial continuous roller imprinting system with controllable mold.

4. Results and Discussion

4.1. Comprehensive Analysis and Discussion on the Mechanical Properties of the Negative Poisson Ratio Structure and Microstructure Mold

4.1.1. Simulation and Analysis on the Influence of Mold Thickness on the Sandwich Polymer Poisson Ratio

Simulation and analysis of the Poisson ratio were conducted via changing 2 mm and 3 mm microstructure thickness of the PDMS mold to a fixed thickness of 10 mm for the TPE's geometric structure and a 10:1 ratio (A:B) for the PDMS mixture. After changing the array structures, the performance of Poisson ratio was stable within the stretching range of elasticity. The results showed that the Poisson ratio had almost doubled in size with a 1 mm increase in PDMS thickness. As the thickness of the PDMS material increases, its Poisson ratio increases accordingly. From a mechanical perspective, due to its sandwich geometry, the driving layer exhibits a negative Poisson ratio. As a result, the thinner PDMS layer is driven and acquires a lower Poisson ratio. Conversely, the thicker PDMS layer is less likely to be pulled outward and has a slightly higher Poisson's ratio, as shown in Table 4.

Table 4. Changes in the Poisson ratio in the sandwich microstructure mold with different mold structure thicknesses.

Thickness of PDMS (mm)	Sandwich Polymer Mold	
	Stretch Length (mm)	Poisson's Ratio
2	1	0.189
	2	0.182
	3	0.183
3	1	0.347
	2	0.358
	3	0.348

4.1.2. Simulation and Analysis of the Influence of PDMS Mold Mixture Ratio on the Sandwich Polymer Poisson Ratio

With a low microstructure PDMS mixture ratio (A:B) of 20:1 and a fixed 2 mm and 3 mm thickness, when the mixture ratio was low, the thickness of the PDMS was 2 mm and 3 mm, which was one order of magnitude lower according to the simulation analysis results of the Poisson ratio, as shown in Table 5. After analyzing the changes in adhesion between PDMS and NPR geometric structure layers with different proportions, it was found that the AB agent with a higher mixing ratio exhibits greater strength and elastic modulus. As a result, it responds more effectively to the tensile variations of the NPR geometric layer and achieves better control accuracy.

Table 5. Influence of the PDMS mold with mixture ratio of 20:1 on the Poisson ratio of the sandwich microstructure mold.

Thickness of PDMS (mm)	Sandwich Polymer Mold	
	Stretch Length (mm)	Poisson's Ratio
2	1	0.016
	2	0.015
	3	0.015
3	1	0.185
	2	0.184
	3	0.184
4	1	0.321
	2	0.320
	3	0.319

4.2. Analysis and Discussion on the Mechanical Properties of the Sandwich Microstructure Mold Applicable for Research

The polymer's intermediate layer was employed as the main driving mode. For driving of the PDMS microstructure layer of the sandwich microstructure mold after recombination, in order to avoid the PPR effect, this study adopted fixed properties for the TPE, and the mechanical properties of the AB agents (the base and curing agent) with unequal proportions on the PDMS microstructure layer were obtained (Table 6) through experiment to meet NPR research demands of the sandwich microstructure mold in this research.

Table 6. Test of the material mechanical properties of different AB agent (base, curing agents) proportions on the PDMS microstructure layer.

Proportion (A:B)	Loading Rate (mm/min)	Tension Stress (MPa)	Modulus (MPa)	Poisson's Ratio	Shear Strength (N/cm^2)
10:1	6	0.165	2.35	0.49	177.25
15:1	6	0.101	1.68	0.46	58.78
20:1	6	0.034	0.63	0.42	15.92

Furthermore, the proportion of AB agents applicable for this research was discussed. This study adopted the NPR structure layer of the TPE with a fixed thickness of 10 mm. Meanwhile, the thickness of the PDMS microstructure layer was set to 1 mm. Different proportions of AB agents (10:1, 15:1, 20:1) were employed to analyze and discuss (Figure 9).

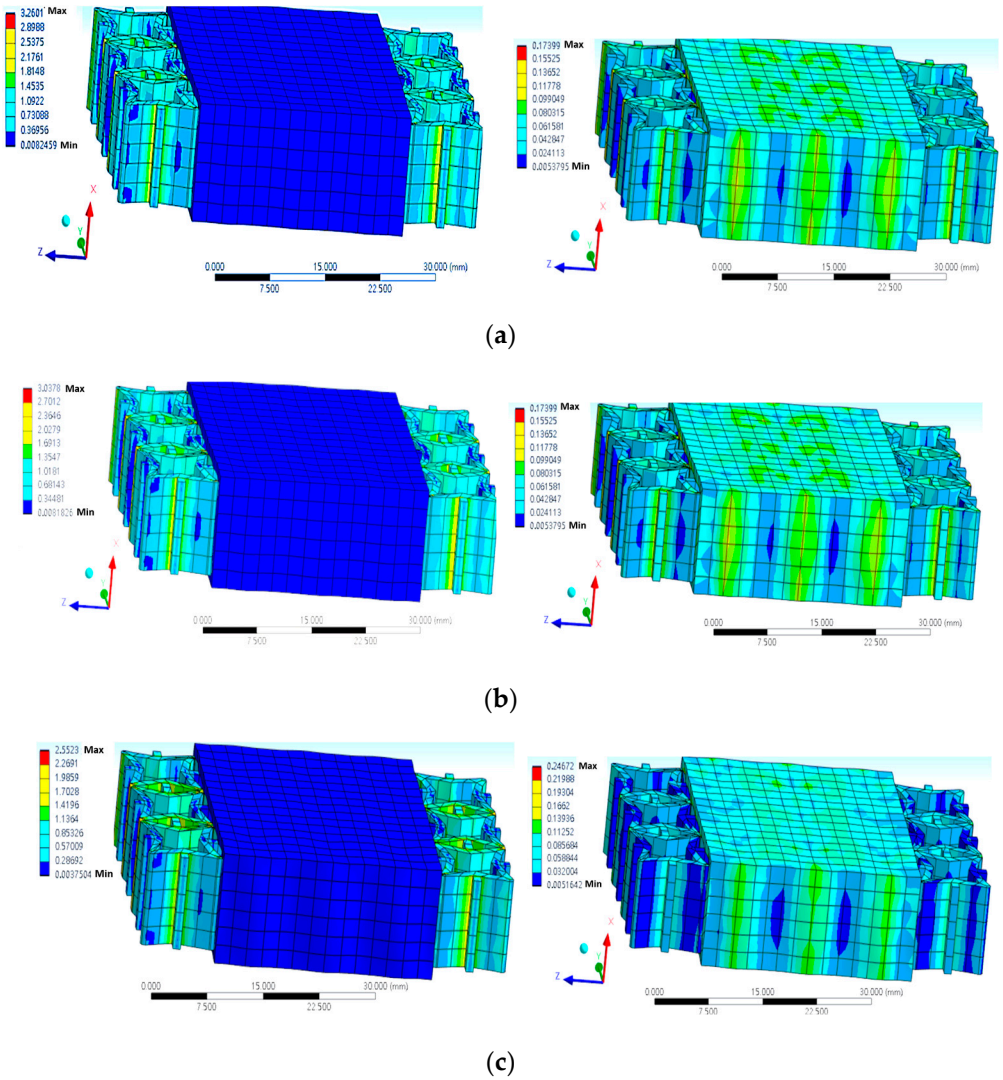


Figure 9. Distribution simulation of the stress–strain diagram for the sandwich microstructure mold in PDMS with different AB agent proportions: (**a**) 10:1; (**b**) 15:1; (**c**) 20:1.

The numerical simulation results showed that different proportions of the AB agents had stable tensile stress–strain diagrams under the same geometric conditions, but that a 20:1 proportion had more stable NPR performance (Figure 10) and a Poisson ratio within the range of −0.2247 to −0.2254. Thus, 20:1 was taken as the proportion in the subsequent PDMS microstructure mold research.

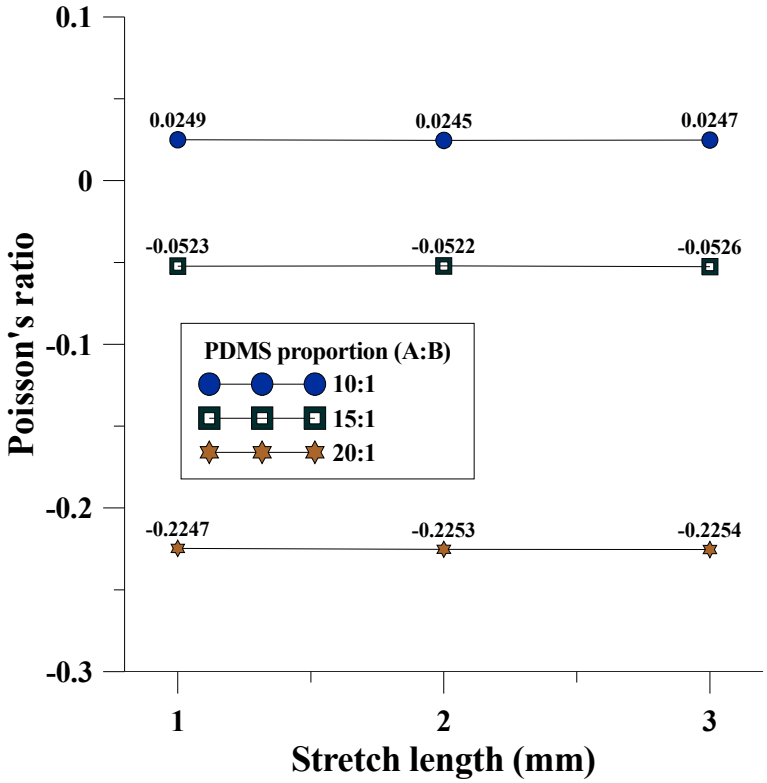


Figure 10. PDMS microstructure mold Poisson ratio performance of the sandwich microstructure mold in PDMS with different AB agent proportions (10:1, 15:1, 20:1).

4.3. Microstructure Structure Adjustment and Discussion on Research System Replication Formability

4.3.1. Sandwich Mold Adjustment and Discussion on Imprinting Replication Formability

This study investigated the NPR structure layer through adjusting and controlling the applicable parameters after obtaining the predicted changed shape of the microstructure, having stretched the microstructure mold of the NPR layer in its (a) original form and by (b) 1 mm, (c) 3 mm, and (d) 5 mm, and then conducted imprinting and replication using the self-developed system, as shown in Table 7 and Figure 11.

Table 7. Influence of the stretch microstructure mold of NPR layer of microstructure deformation.

Stretch Length (mm)	Microstructure Feature Size	
	Diameter (mm)	Hight (mm)
0	208.2	89.92
1	209.5	89.73
3	210.8	89.41
5	211.6	88.37

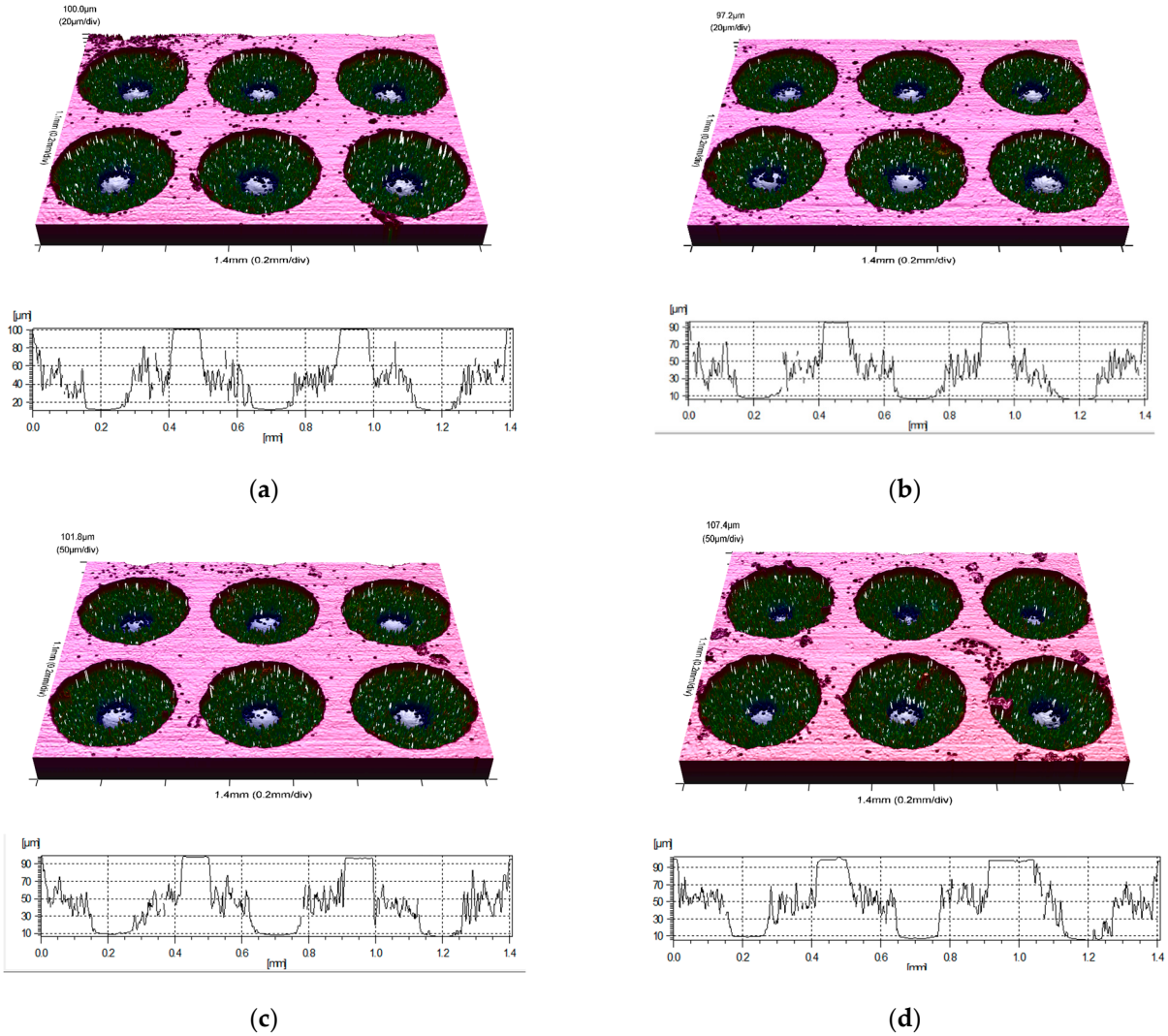


Figure 11. Stretch microstructure mold of NPR layer (**a**) original (**b**) 1 mm (**c**) 3 mm (**d**) 5 mm.

The experiment results showed that the shape of the microstructure reached the changes required by the pre-simulation by adjusting the stretching. This section was compared with the previous Table 7, examining the influence of the stretched microstructure mold on the NPR layer's microstructure deformation after experiments and white light measurements. Meanwhile, the high replication formability of the microstructure obtained through white light scanning after subsequent roller imprinting was up to 98.75%. The diameter of microstructure reached 99.025%. Highly effective imprinting and replication properties could therefore be obtained in comparison with the previous mold, as shown in Figure 12. In 2008, Grimes et al. [20] used biaxially stretched polystyrene with prestressed shrinkage properties and successfully applied heating to reduce the microstructure size from 800 μm to 300 μm. Compared to previous related studies, this research proposed a new successful method for controlling microstructures. During the research process, the printing density of the NPR structure produced in the 3D printing system may influence certain mechanical properties. A higher density enhances characteristic behavior, making it necessary to standardize the experimental printing density. Printing defects in low-density structures can affect stretching control. Additionally, the printing speed should be reduced to ensure complete and sufficient molding, preventing adhesion or deformation issues.

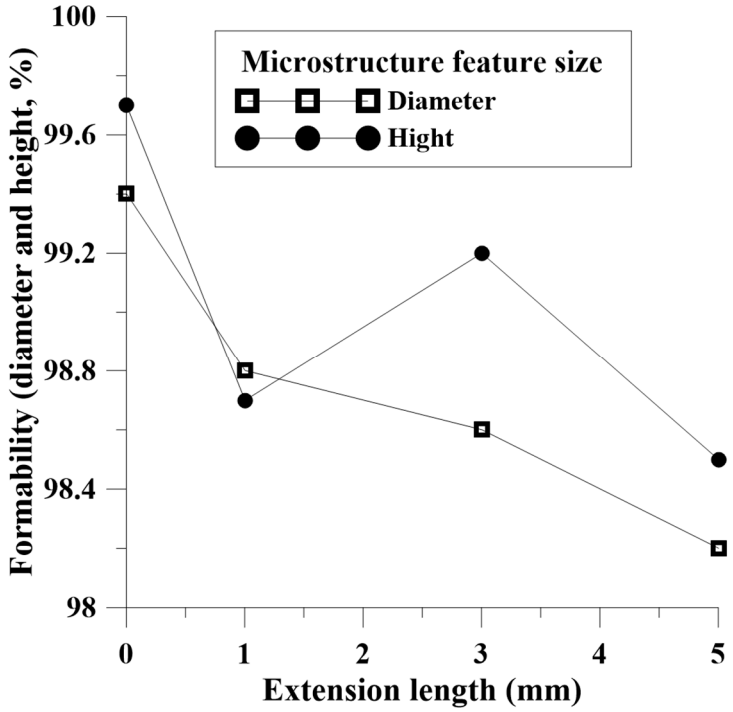


Figure 12. Formability of imprinting and replication of the sandwich mold.

4.3.2. Analysis on Microstructure Optical Detection

This study conducted optical detection on the array microstructure after replication and imprinting by shining a high-strength laser source on the microstructure. Meanwhile, the stability of imprinting and replication and the consistency of the microstructure were judged via passing a light spot on the microstructure. The results proved that the focusing effect of the replicated microstructure was stable through detection, as shown in Figure 13.

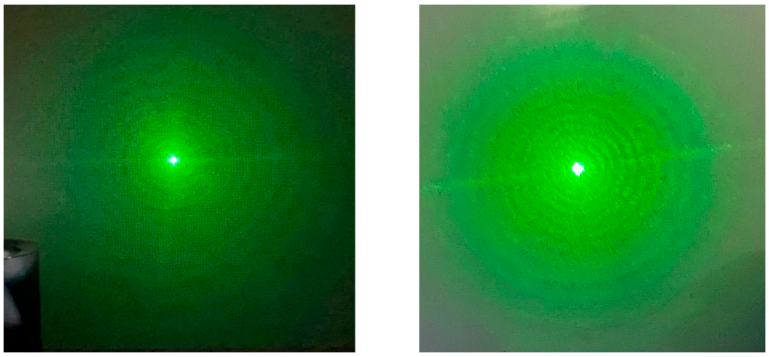


Figure 13. Image of optical focus detection in replicated array microstructures.

4.3.3. Discussion on the Limitations and Scalability of the Proposed Process

In this study, the regulation range of the soft mold is determined by the microstructural scale, depending on the researcher's illustrations relating to the geometric layer of unit geometry graph dimensions. This framework defines the control range within the elastic deformation limits and a comprehensive evaluation of the mechanical elasticity of the selected materials; researchers require such material parameters and fundamental criteria for experimental execution. Additionally, environmental parameters must be carefully considered as they may significantly influence the mechanical properties of polymer-based soft molds during the imprint molding process.

5. Conclusions

This research put forward roller imprinting replication processing technology with an octagonal starfish geometric structure and a multi-space and multi-axial controllable microstructure mold. Roller imprinting was conducted by setting up a new roller imprinting system with a multi-space and multi-axial controllable mold, and the octagonal starfish geometric structure was designed as a method to control deformation of the microstructure. Metallic and polymer molds were compared first, and a thermoplastic elastomer (TPE) was finally selected as the material for designing the geometric patterns in this research. The best negative Poisson ratio range for the sandwich microstructure mold (1 mm thickness of PDMS microstructure layer is as thickness setting for discussion in this part, 20:1 proportion of AB agents show comparatively stable NPR performance and Poisson ratio is within the range of -0.2247–-0.2254) was obtained through simulation and analysis. After several attempts, a sandwich microstructure mold was made. Continuous roll imprinting processing was realized based on systematic steps. The results proved that the high replication formability of the microstructure obtained through white light scanning after subsequent roller imprinting was up to 98.75%. The diameter of microstructure reached 99.025%, and the development of this innovative system and method of new technology could obtain the expected replication formability of the microstructure.

Author Contributions: Conceptualization, Y.-J.W.; methodology, Y.-J.W., Y.-X.Z., J.-C.G. and Z.-J.W., software, Y.-J.W., Y.-X.Z., J.-C.G. and Z.-J.W.; writing—review and editing, Y.-J.W. All authors have read and agreed to the published version of the manuscript.

Funding: This work was partially supported by the National Science and Technology Council (Series No. NSTC 112-2221-E-415-014 and NSTC 113-2221-E-415-001) of Taiwan, Republic of China.

Data Availability Statement: The raw data supporting the conclusions of this article will be made available by the authors on request.

Acknowledgments: This work was partially supported by the National Science and Technology Council (Series No. NSTC 112-2221-E-415-014 and NSTC 113-2221-E-415-001) of Taiwan, ROC. A preliminary summary of the initial research concept was first presented at the 2024 International Polymer Engineering and Science Conference, held in Tokyo in July 2024.

Conflicts of Interest: The authors declare no conflicts of interest.

References

1. Wang, J.; Wang, H.; Lai, L.; Li, Y. Preparation of microneedle array mold based on MEMS lithography technology. *Micromachines* **2020**, *12*, 23. [CrossRef] [PubMed]
2. Yahagi, T.; Murayama, H.; Watanabe, Y.; Mineta, T. Fabrication of MEMS mold with inclined micro-multi-fin structure and shape transfer to resin by thermal imprint process. *Jpn. J. Appl. Phys.* **2020**, *59*, SIIJ02. [CrossRef]
3. Ansari, A.; Trehan, R.; Watson, C.; Senyo, S. Increasing silicone mold longevity: A review of surface modification techniques for PDMS-PDMS double casting. *Soft Mater.* **2021**, *19*, 388–399. [CrossRef] [PubMed]
4. Zhou, T.; He, Y.; Wang, T.; Zhu, Z.; Xu, R.; Yu, Q.; Zhao, B.; Zhao, W.; Liu, P.; Wang, X. A review of the techniques for the mold manufacturing of micro/nanostructures for precision glass molding. *Int. J. Extrem. Manuf.* **2021**, *3*, 042002. [CrossRef]
5. You, K.; Fang, F.; Yan, G.; Zhang, Y. Experimental investigation on laser assisted diamond turning of binderless tungsten carbide by in-process heating. *Micromachines* **2020**, *11*, 1104. [CrossRef] [PubMed]
6. Acherjee, B. State-of-art review of laser irradiation strategies applied to laser transmission welding of polymers. *Opt. Laser Technol.* **2021**, *137*, 106737. [CrossRef]
7. Weng, Y.J.; Huang, J.C.; Chen, Y.Y.; Hsu, S.T.; Zhang, Z.R. A study on the dynamic forming mechanism development of the negative Poisson's ratio elastomer molds—Plate to plate (P2P) forming process. *Polymers* **2021**, *13*, 3255. [CrossRef] [PubMed]
8. Supreeti, S. Soft Nanoimprint Lithography on Curved Surfaces. Doctoral Dissertation, TU Ilmenau, Ilmenau, Germany, 2020.
9. Ryan, K.R.; Down, M.P.; Hurst, N.J.; Keefe, E.M.; Banks, C.E. Additive manufacturing (3D imprinting) of electrically conductive polymers and polymer nanocomposites and their applications. *EScience* **2022**, *2*, 365–381. [CrossRef]

10. Su, R.; Wen, J.; Su, Q.; Wiederoder, M.S.; Koester, S.J.; Uzarski, J.R.; McAlpine, M.C. 3D printed self-supporting elastomeric structures for multifunctional microfluidics. *Sci. Adv.* **2020**, *6*, eabc9846. [CrossRef] [PubMed]
11. Scott, S.M.; Ali, Z. Fabrication methods for microfluidic devices: An overview. *Micromachines* **2021**, *12*, 319. [CrossRef] [PubMed]
12. Khonina, S.N.; Voronkov, G.S.; Grakhova, E.P.; Kazanskiy, N.L.; Kutluyarov, R.V.; Butt, M.A. Polymer waveguide-based optical sensors—Interest in bio, gas, temperature, and mechanical sensing applications. *Coatings* **2023**, *13*, 549. [CrossRef]
13. Soldera, M.; Wang, Q.; Soldera, F.; Lang, V.; Abate, A.; Lasagni, A.F. Toward high-throughput texturing of polymer foils for enhanced light trapping in flexible perovskite solar cells using roll-to-roll hot embossing. *Adv. Eng. Mater.* **2020**, *22*, 1901217. [CrossRef]
14. Handrea-Dragan, M.; Botiz, I. Multifunctional structured platforms: From patterning of polymer-based films to their subsequent filling with various nanomaterials. *Polymers* **2021**, *13*, 445. [CrossRef]
15. Deshmukh, S.S.; Goswami, A. Hot embossing of polymers–A review. *Mater. Today Proc.* **2020**, *26*, 405–414. [CrossRef]
16. Zhang, H.; Ding, B.; Chen, T. A high efficiency industrial polysilicon solar cell with a honeycomb-like surface fabricated by wet etching using a photoresist mask. *Appl. Surf. Sci.* **2016**, *387*, 1265–1273. [CrossRef]
17. Nguyen, H.T.; Lee, Y.C. Step and scanning lithography for patterning seamless microstructures on the inner surface of a hollow roller. *J. Micromech. Microeng.* **2019**, *29*, 105012. [CrossRef]
18. Kang, M.A.; Kim, S.J.; Song, W.; Chang, S.J.; Park, C.Y.; Myung, S.; Lim, J.; Lee, S.S.; An, K.S. Fabrication of flexible optoelectronic devices based on MoS2/graphene hybrid patterns by a soft lithographic patterning method. *Carbon* **2017**, *116*, 167–173. [CrossRef]
19. MatWeb, L.L.C. Material Property Data. MatWeb. Available online: https://asia.matweb.com/search/SearchProperty.asp?e=1 (accessed on 1 March 2025).
20. Grimes, A.; Breslauer, D.N.; Long, M.; Pegan, J.; Lee, L.P.; Khine, M. Shrinky-Dink microfluidics: Rapid generation of deep and rounded patterns. *Lab Chip* **2008**, *8*, 170–172. [CrossRef]

Disclaimer/Publisher's Note: The statements, opinions and data contained in all publications are solely those of the individual author(s) and contributor(s) and not of MDPI and/or the editor(s). MDPI and/or the editor(s) disclaim responsibility for any injury to people or property resulting from any ideas, methods, instructions or products referred to in the content.